Check for updates

FEBS Letters

FEBS PRESS science publishing by scientists

Selective increment of phosphatidylserine on the autophagic body membrane in the yeast vacuole

Yuki Yamakuchi[1], Yuna Kurokawa[1], Rikako Konishi[1], Kayoko Fukuda[1], Tatsunori Masatani[2,‡] and Akikazu Fujita[1]

1 Department of Molecular and Cell Biology and Biochemistry, Basic Veterinary Science, Faculty of Veterinary Medicine, Kagoshima University, Kagoshima, Japan

2 Transboundary Animal Diseases Research Center, Joint Faculty of Veterinary Medicine, Kagoshima University, Kagoshima, Japan

Correspondence

A. Fujita, Department of Molecular and Cell Biology and Biochemistry, Basic Veterinary Science, Faculty of Veterinary Medicine, Kagoshima University, Korimoto 1-21-24, Kagoshima 890-0065, Japan

Tel: +81 99 285 8714

E-mail: afujita@vet.kagoshima-u.ac.jp

Present address

‡Laboratory of Zoonotic Diseases, Faculty of Applied Biological Sciences, Gifu University, Gifu, Japan

(Received 6 May 2021, revised 15 July 2021, accepted 21 July 2021, available online 14 August 2021)

doi:10.1002/1873-3468.14167

Edited by Hitoshi Nakatogawa

In yeast cells, the autophagosome is a double-membrane structure; the inner membrane becomes the autophagic body membrane in the vacuole. Vacuolar enzymes degrade the autophagic body. There is no critical information regarding its selective degradation. Using the electron microscopy method, distributions of four phospholipids were examined in the autophagosomal and autophagic body membranes upon autophagy induction. The labeling of phosphatidylserine (PtdSer) in the autophagic body membrane dramatically increased after it converted from the autophagosome, but remained low in the vacuolar membrane. PtdSer in the autophagic body membrane also increased in *atg15*Δ yeast. These results suggest that the selective increment of PtdSer in the autophagic body, but not the vacuolar, membrane, can explain the selective degradation of the autophagic membrane.

Keywords: autophagy; electron microscopy; freeze fracture; lipids; nanoscale; phosphatidylcholine; phosphatidylserine; phosphoinositide

Macroautophagy (autophagy) is an intracellular degradation system and plays essential roles in a broad range of physiological functions [1]. Defects in the autophagy signaling process result in various diseases, such as Parkinson's disease [2–5] and Crohn's disease [6]. During autophagy, an initial membrane structure, known as the isolation membrane or phagophore, appears in the cytoplasm and extends and encloses a portion of the cytosol and/or organelles to finally mature into double-membrane structures known as autophagosomes. The autophagosome fuses with the vacuole in yeast and plants (also called a lysosome in mammalian cells) to engulf cytoplasmic contents as an autophagic body in yeast derived from the inner part of two autophagosomal membranes. Subsequently, the enzymes in the vacuolar lumen selectively degrade the autophagic body membrane and cytoplasmic contents, but not the vacuolar membrane, to reuse the metabolites as nutrients in the yeast cell. The vacuolar membrane is resistant to hydrolytic attack from its own enzymes. Compared with the initial stages of autophagy, the mechanism and regulation of the selective degradation of the autophagic body, but not the vacuolar membrane, are very poorly investigated and less understood.

Abbreviations

EF, E-face (exoplasmic or luminal leaflet); EM, electron microscopy; GST, glutathione S-transferase; LTP, lipid transfer protein; OSBP, oxysterol-binding protein; PF, P-face (protoplasmic or cytoplasmic leaflet); PH, pleckstrin homology; PLC, phospholipase C; PMSF, phenylmethylsulfonyl fluoride; PtdCho, phosphatidylcholine; PtdIns(3)P, phosphatidylinositol 3-phosphate; PtdIns(4)P, phosphatidylinositol 4-phosphate; PtdIns(4,5)P_2, phosphatidylinositol 4,5-bisphosphate; PtdSer, phosphatidylserine; PX, phox homology; QF, quick freezing; QF-FRL, quick-freezing and freeze-fracture replica labeling.

18733468, 2021, 17, Downloaded from https://febs.onlinelibrary.wiley.com/doi/10.1002/1873-3468.14167 by CochraneChina, Wiley Online Library on [02/03/2023]. See the Terms and Conditions (https://onlinelibrary.wiley.com/terms-and-conditions) on Wiley Online Library for rules of use; OA articles are governed by the applicable Creative Commons License

In this study, a quick-freezing and freeze-fracture replica labeling (QF-FRL) method was employed to examine the distribution of four lipids in the autophagosome, autophagic body, and vacuolar membranes. Using this method, we could analyze the membrane lipid distribution at the nanoscale level by physically fixing the membrane molecules. In this method, cells were quickly frozen, and membrane halves split at the hydrophobic interface were cast by vacuum evaporation of carbon and platinum. Thus, membrane lipids were physically stabilized, and the exposed hydrophilic heads could be labeled without artificial perturbations. In this study, using the QF-FRL method, phosphatidylserine (PtdSer) was increased in the autophagic body membrane in the vacuole, but not in the limiting membrane of the vacuole. From these results, we could elucidate the selective degradation mechanisms of the autophagic body in yeast's vacuole.

Materials and methods

Reagents

Propargylcholine bromide and biotin-azide were purchased from Aobious, Inc. (Gloucester, MA, USA) and Invitrogen (Carlsbad, CA, USA), respectively.

Probes

cDNA generated by RT-PCR of HEK293 cell total RNA was used as a template to clone the PH domain of OSBP and the PX domain of p40Phox. The plasmid containing the PHx2 domain of Evectin-2 was kindly provided by Dr. Tomohiko Taguchi (Tohoku University, Japan) and Dr. Takuma Kishimoto (Hokkaido University, Japan). Recombinant GST fusion proteins containing the OSBP PH domain (GST-OSBP-PH), p40Phox PX domain (GST-p40Phox-PX), Evectin-2 PH domain (GST-Evectin-2-PH), and PLC-δ1 PH domain (GST-PLC-PH) were expressed in *Escherichia coli* and purified, as described previously [8,25]. The PH domain of PLC-δ1 was obtained from the GST-PLC-PH domain fusion protein by cleavage with PreScission Protease (GE Healthcare Life Sciences, Pittsburgh, PA, USA), according to the manufacturer's protocol. Secondary rabbit anti-GST antibody was purchased from Bethyl Laboratories (Montgomery, TX, USA), and 10 nm gold particle-conjugated anti-mouse IgG and anti-rabbit IgG antibodies were purchased from BioCell (Cardiff, UK).

Yeast

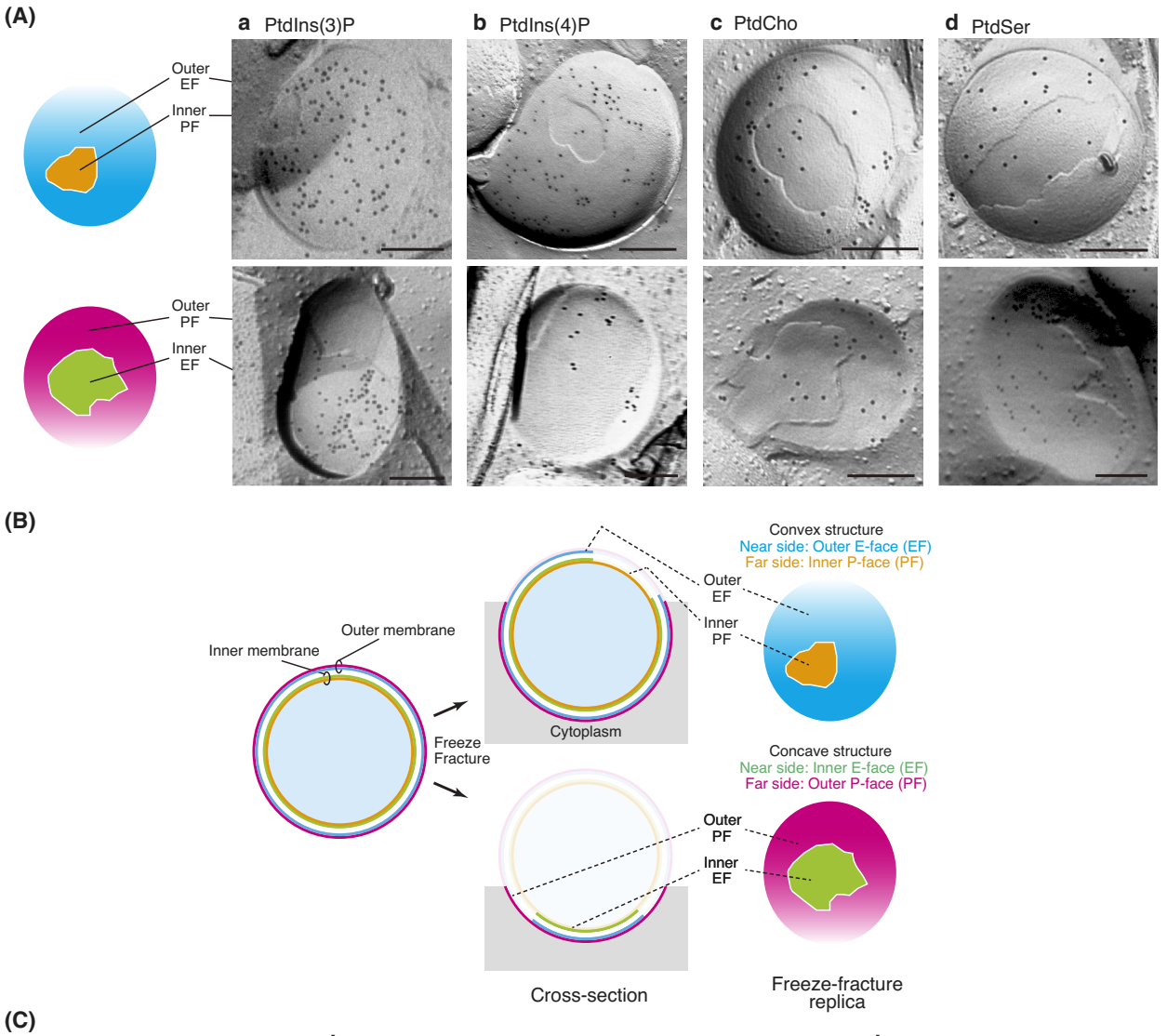
Cells were grown in YPD medium (1% yeast extract, 2% Bacto Peptone, and 2% dextrose) at 30 °C and harvested during the transition to the exponential or stationary phase. To label PtdCho, yeast cells were cultured in YPD containing 1 mM propargylcholine bromide and used in the log phase [10]. All yeast strains used in this study were based on the parent strain, *Saccharomyces cerevisiae* SEY6210 (*MATα leu2-3, 112 ura3-52 his3-Δ200 trpl-Δ901 lys2-801 suc2Δ9 GAL*; Table S1). Deletion mutants were generated using a PCR-based method using pUG6 plasmids as templates [26]. To induce autophagy, wild-type, *atg15*Δ, and *pep4*Δ yeasts cultured in YPD medium were washed with water and incubated for 5 h at 30 °C in a nitrogen and carbon-deleted medium [S(-NC); 0.17% yeast nitrogen base without amino acids and ammonium sulfate; Becton Dickinson]. The S(-NC) medium was supplemented with 1 mM PMSF (Sigma, St. Louis, MO, USA) for wild-type, but not *atg15*Δ or *pep4*Δ, yeast strains. In this study, S(-NC) supplemented with 1 mM PMSF was used, which is a well-known proteinase inhibitor, when autophagy in the yeast cell was induced to leave autophagic bodies intact to observe them in the vacuole.

QF and freeze-fracture

Quantitative lipid labeling of the biological membranes of budding yeast cells was performed either by QF yeast cells using a metal sandwich QF method or by high-pressure freezing using an HPM 010 high-pressure freezing machine (Leica Microsystems, Wetzlar, Germany). For metal sandwich freezing, a small volume of yeast pellet was placed on a copper foil,

Fig. 1. Localizations of PtdIns(3)P, PtdIns(4)P, PtdCho, and PtdSer in the autophagosome membrane in budding yeast. (A) Autophagosomes in wild-type (WT) yeast cultures in S(-NC) medium for 5 h. Autophagosomes were identified as a smooth-surfaced double-membrane structure, seen in two different patterns, as shown in (B). The top panel shows the convex structures displaying the outer membrane EF and the inner membrane PF. The bottom panel shows the concave structures displaying the outer membrane PF and the inner membrane EF. As reported previously, for PtdIns(3)P (Aa) and PtdIns(4)P (Ab), both labelings on the EF were higher than those on the PF. In contrast, the labelings of PtdCho and PtdSer were detected in both EF and PF of both inner and outer membranes with similar densities. Scale bar, 200 nm. (B) Membrane topologies of autophagosomes in freeze-fracture electron microscopy. Autophagosomes are observed as smooth-surfaced double-membrane structures in the cytoplasm. The outer and inner membranes can be distinguished based on the convexity or concavity of the structure and whether the membrane appears as the near-side or far-side layer. (C) Labeling density of each phospholipid in WT yeast cultured in S(-NC) medium for 5 h (average ± SEM). The labeling densities of PtdIns(3)P (a) and PtdIns(4)P (b) on the EF were higher than those on the PF in both outer and inner autophagosomal membranes. The labeling densities of PtdCho and PtdSer on EF were comparable to those in PF in both inner and outer membranes. Experiments were done more than three times, and the number of colloidal gold particles per square micrometer was measured in >10 randomly selected images.

18733468, 2021, 17, Downloaded from https://febs.onlinelibrary.wiley.com/doi/10.1002/1873-3468.14167 by CochraneChina, Wiley Online Library on [02/03/2023]. See the Terms and Conditions (https://onlinelibrary.wiley.com/terms-and-conditions) on Wiley Online Library for rules of use; OA articles are governed by the applicable Creative Commons License



covered with a thin gold foil (~ 4 mm^2 in area; 20 μm thick), and frozen by a quick press between two gold-plated copper blocks precooled in liquid nitrogen [25,27]. For high-pressure freezing, an EM grid (200 mesh) impregnated with yeast cells was sandwiched between a flat aluminum disk (Engineering Office M. Wohlwend, Sennwald, Switzerland) and frozen according to the manufacturer's instructions [9].

For freeze-fracture, frozen specimens were transferred to the cold stage of a Balzers BAF400 apparatus (Bal-Tec AG; Balzers, Liechtenstein) and fractured at −130 °C

18733468, 2021, 17, Downloaded from https://febs.onlinelibrary.wiley.com/doi/10.1002/1873-3468.14167 by CochraneChina, Wiley Online Library on [02/03/2023]. See the Terms and Conditions (https://onlinelibrary.wiley.com/terms-and-conditions) on Wiley Online Library for rules of use; OA articles are governed by the applicable Creative Commons License

under a vacuum of ~ 1×10^{-6} mbar. Replicas were made by electron-beam evaporation in three steps: carbon (~ 3 nm thick) at an angle of 90° to the specimen surface, platinum-carbon (1–2 nm) at an angle of 45°, and carbon (10–20 nm) at an angle of 90 °, as described previously [28]. The deposition thickness was adjusted by referring to a crystal thickness monitor (EM QSG100; Leica Microsystems, Lahn-Dill-Kreis, Hesse, Germany).

Thawed specimens were incubated with 2.5% SDS in 0.1 M Tris/HCl (pH 8.0) at 60 °C to 70 °C overnight. To remove the cell wall, yeast replicas were digested with 1 mg·mL^{-1} Zymolyase 20T in PBS containing 0.1% Triton X-100, 1% BSA, and a protease inhibitor cocktail (Nacalai Tesque) for 2 h at 37 °C. After further treatment with 2.5% SDS, the replicas were stored in buffered 50% glycerol at −30 °C until use.

Labeling and EM observation

Labeling with probes was performed as previously described [28]. Briefly, after rinsing, freeze-fracture replicas were blocked with PBS containing 2% cold water fish skin gelatin at room temperature (18 ~ 25 °C) for 30 min. The samples were incubated at 4 °C overnight with 40 ng·mL^{-1} GST-OSBP-PH, 30 ng·mL^{-1} GST-p40Phox-Phox homology (PX), or 20 μg·mL^{-1} GST-Evectin-2-PH in PBS containing 2% cold water fish skin gelatin. Then, the samples were successively incubated in PBS containing 2% cold water fish skin gelatin at 37 °C for 30 min each with a rabbit anti-GST antibody (5 μg·mL^{-1}) and 50-fold diluted colloidal gold (10 nm)-conjugated anti-rabbit IgG antibody (EM.GFAR 10; BBI Solutions, Cardiff, UK). To block the nonspecific binding of GST-OSBP-PH to PtdIns(4,5)P_2, the replicas were pretreated with the PH domain (1 mg·mL^{-1}) of PLC-δ1 in the blocking solution [25]. The replicas were then incubated with primary probes diluted in PBS containing 2% cold water fish skin gelatin at 4 °C overnight. After four washes with PBS containing 0.1% BSA, the replicas were incubated with 10 nm gold-conjugated secondary antibody in PBS containing 2% cold water fish skin gelatin at 37 °C for 30 min.

PtdCho in the biological membrane of yeast cells was labeled using the click chemistry method, as described previously [10]. Briefly, yeast was cultured overnight in YPD medium supplemented with 1 mM propargylcholine bromide, and the replicas of the yeast cells were incubated in 0.1 M Tris/HCl (pH 7.4) containing 1 mM $CuSO_4$, 0.1 M ascorbic acid, and 10 μM biotin-azide for 30 min at 37 °C. After rinsing, the replicas were blocked with 3% (w/v) BSA in PBS-Tween 20 for 30 min at room temperature and incubated with mouse anti-biotin (10 μg·mL^{-1}) in 1% BSA in PBS at 4 °C overnight, followed by incubation with goat anti-mouse IgG antibody conjugated with 10 nm colloidal gold for 30 min at 37 °C in 1% BSA in PBS. The replicas were picked up on Formvar-coated grids and observed with an H7650 EM (Hitachi, Tokyo, Japan) operated at 80 kV.

Statistical analysis

Each experiment was performed at least thrice. The areas in the images were measured using Fiji (IMAGEJ), and the labeling density was indicated as the number of colloidal gold particles in 1 μm^2. For each structure, the labeling density was measured in > 10 randomly selected images. Statistical differences between samples were tested using Student's *t*-test.

Results and discussion

Labeling of phosphatidylinositol 4-phosphate [PtdIns(4)P] by the pleckstrin homology (PH) domain of the oxysterol-binding protein (OSBP)

In our previous report [7], we found that phosphatidylinositol (Ptd) 4-kinases Pik1p and Stt4p play essential and distinct roles in yeast autophagy. We also showed that the labeling of anti-PtdIns(4)P antibody was abundantly localized on the luminal leaflet or the E-face (EF) in both the outer and inner membranes of the autophagosome. On the contrary, PtdIns(4)P labeling was not detected in the autophagic body membrane in the vacuole, which is derived from the inner membrane of the autophagosome. We believe that dynamic changes in PtdIns(4)P levels in the membrane of the autophagosome and the autophagic body play key roles in the regulation of autophagic body membrane conditions. We developed a labeling method for PtdIns(4)P in this study using another probe to confirm the level of PtdIns(4)P in the membrane of the autophagosome and the autophagic body. The recombinant glutathione S-transferase (GST)-tagged PH domain of human OSBP (GST-OSBP-PH) was used to label PtdIns(4)P in the freeze-fracture replica. To confirm the binding specificity of the GST-OSBP-PH to PtdIns(4)P, replicas of liposomes composed of 95 mol% phosphatidylcholine (PtdCho) and 5 mol% of phospholipids (PtdA, PtdSer, PtdEth, PtdIns, PtdIns(3)P, PtdIns(4)P, PtdIns(5)P, PtdIns(3,4)P_2, PtdIns(3,5)P_2, PtdIns(4,5)P_2, and PtdIns(3,4,5)P_3) were labeled. These freeze-fracture replicas were incubated with GST-OSBP-PH, followed by rabbit GST antibody and 10 nm colloidal gold-conjugated anti-rabbit IgG antibody. Considerable labeling of GST-OSBP-PH was detected in the PtdIns(4)P-containing liposome replica; however, significant labeling was also observed in the phosphatidylinositol 4,5-bisphosphate [PtdIns(4,5)P_2] liposome replica (Fig. S1A and C). The labeling density per unit area was 60 and 20 times higher in liposomes containing PtdIns(4)P and PtdIns(4,5)P_2, respectively, than that in the other 10 liposome replicas (Fig. S1A and C). To inhibit the binding to PtdIns(4,5)P_2 by GST-OSBP-PH, the replicas

18733468, 2021, 17, Downloaded from https://febs.onlinelibrary.wiley.com/doi/10.1002/1873-3468.14167 by CochraneChina, Wiley Online Library on [02/03/2023]. See the Terms and Conditions (https://onlinelibrary.wiley.com/terms-and-conditions) on Wiley Online Library for rules of use; OA articles are governed by the applicable Creative Commons License

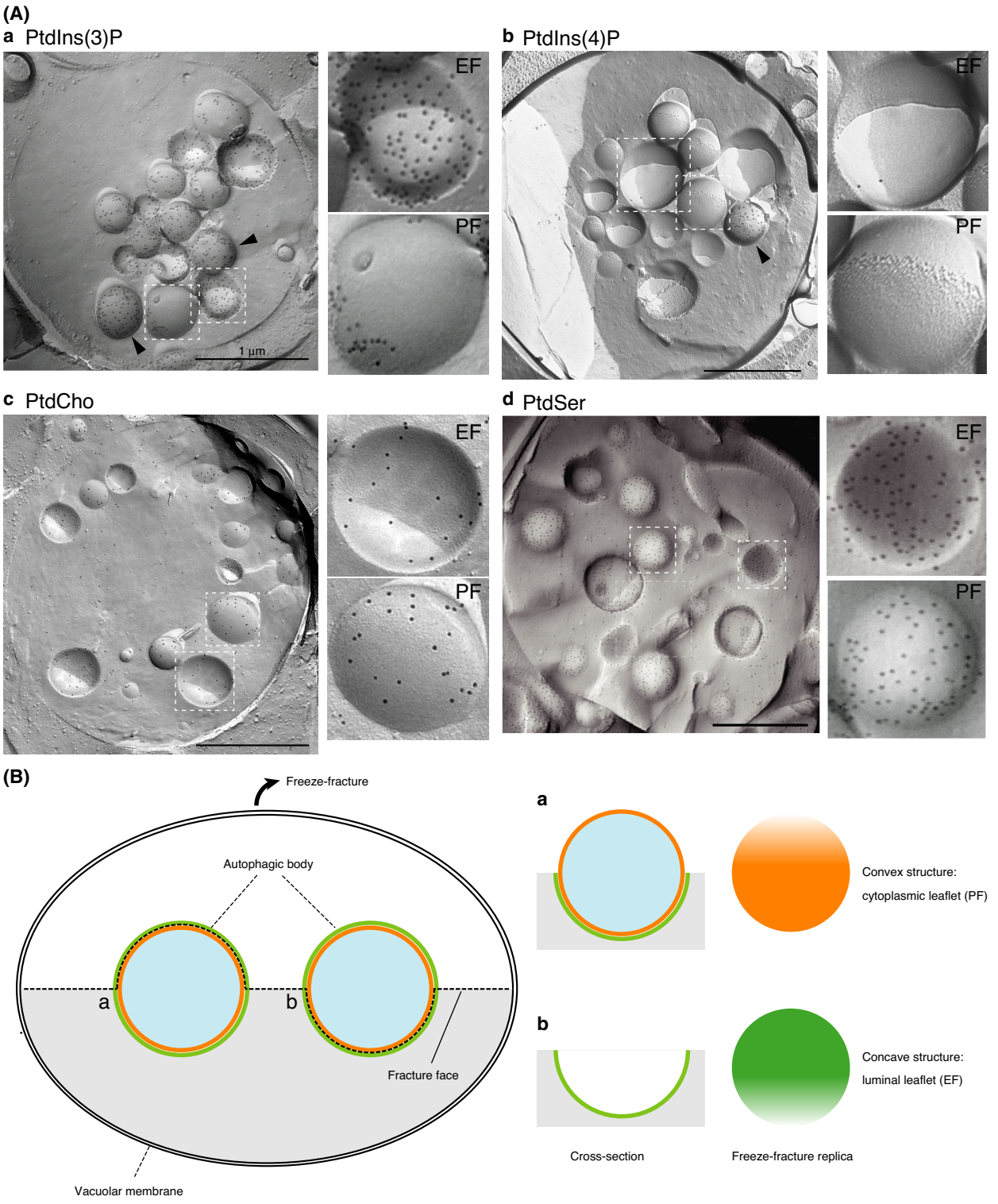


Fig. 2. PtdIns(3)P, PtdIns(4)P, PtdCho, and PtdSer in the yeast autophagic body membrane. (A) Wild-type (WT) yeast cultured in S(-NC) medium for 5 h. Although no labeling of PtdIns(4)P was detected in the EF of the autophagic body membrane in the vacuolar lumen in general (Ab), the intense labelings of PtdIns(3)P (Aa), PtdCho (Ac), and PtdSer (Ad) were observed on the EF. Intense labeling in the PF of the lipophagic vesicle was observed (arrowheads in Aa and Ab). Scale bar, 1 μm. (B) Membrane topologies of autophagic bodies in freeze-fracture electron microscopy. Autophagic bodies are observed as single-membrane structures in the vacuolar lumen. When an autophagic body appears as a convex structure, the observed layer is the PF (a); when it appears as a concave structure, the observed layer is the EF (b).

18733468, 2021, 17, Downloaded from https://febs.onlinelibrary.wiley.com/doi/10.1002/1873-3468.14167 by CochraneChina, Wiley Online Library on [02/03/2023]. See the Terms and Conditions (https://onlinelibrary.wiley.com/terms-and-conditions) on Wiley Online Library for rules of use; OA articles are governed by the applicable Creative Commons License

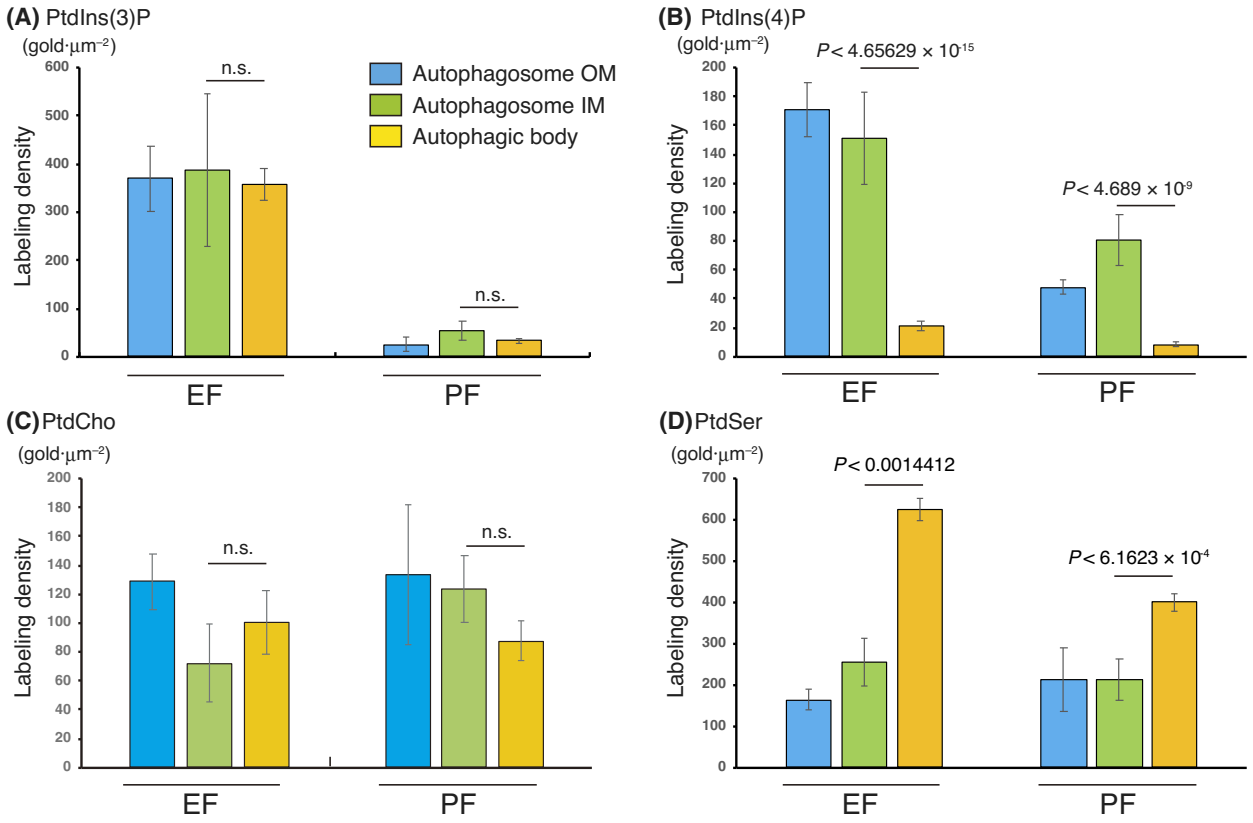


Fig. 3. Labeling densities of PtdIns(3)P, PtdIns(4)P, PtdCho, and PtdSer in the autophagosomal and autophagic body membranes. Labeling gold densities (average ± SEM) of PtdIns(3)P (A), PtdIns(4)P (B), PtdCho (C), and PtdSer (D) in wild-type (WT) yeast cultured in S(-NC) medium for 5 h are shown. The labeling densities of PtdIns(4)P and PtdSer on both EF and PF of the autophagic body were significantly lower and higher than those of the inner autophagosomal membrane, respectively. In contrast to PtdIns(4)P or PtdSer, the labeling densities of PtdIns(3)P and PtdCho on both EF and PF of the autophagic membrane were comparable with those of the autophagosomal membrane. Experiments were repeated three times, and the number of colloidal gold particles per square micrometer was measured in > 20 randomly selected images. Data were obtained from three independent experiments.

were pretreated with the PH domain of phospholipase C (PLC)-δ1 (PLC-PH), which was shown to specifically bind to PtdIns(4,5)P_2 in a previous report [8]. Pretreatment of PLC-PH for 30 min drastically diminished the labeling of PtdIns(4,5)P_2, but not PtdIns(4)P, in the replicas (Fig. S1). In the following experiments, pretreatment with PLC-PH was performed when the freeze-fracture replicas of yeast cells were labeled with GST-OSBP-PH.

Labeling of PtdIns(4)P, phosphatidylinositol 3-phosphate [PtdIns(3)P], PtdCho, and PtdSer in yeast autophagosome

The replica of yeast cells cultured in S(-NC) medium for 5 h with GST-OSBP-PH as a probe was labeled to precisely determine the distribution of PtdIns(4)P in the autophagosome membrane. The labeling of the GST-OSBP-PH, indicating PtdIns(4)P, was abundantly localized on both the E-face (EF; representing the luminal leaflet) and P-face (PF; representing the cytoplasmic leaflet) of the inner and outer membranes of autophagosomes (Fig. 1Ab, B, Cb). The labeling density was significantly higher in the EF than in the PF of both the inner and outer autophagosomal membranes. These results were consistent with those of a previous study in which the replica was labeled with the anti-PtdIns(4)P antibody [7]. PtdIns(3)P labeling by GST-p40Phox-PX was also detected on both EF and PF in both the outer and inner membranes of the autophagosome (Fig. 1Aa and Ca), and the labeling density on the EF was significantly higher than the PF of both inner and outer autophagosomal membranes, which is consistent with a previous report [9]. PtdCho in the autophagosomal membrane was labeled using the click chemistry reaction, as described previously [10], and for the labeling of PtdSer, we used a GST-Evectin-2-PH fusion protein as a probe [11] (see also 'Materials and METHODS'). In

18733468, 2021, 17, Downloaded from https://febs.onlinelibrary.wiley.com/doi/10.1002/1873-3468.14167 by CochraneChina, Wiley Online Library on [02/03/2023]. See the Terms and Conditions (https://onlinelibrary.wiley.com/terms-and-conditions) on Wiley Online Library for rules of use; OA articles are governed by the applicable Creative Commons License

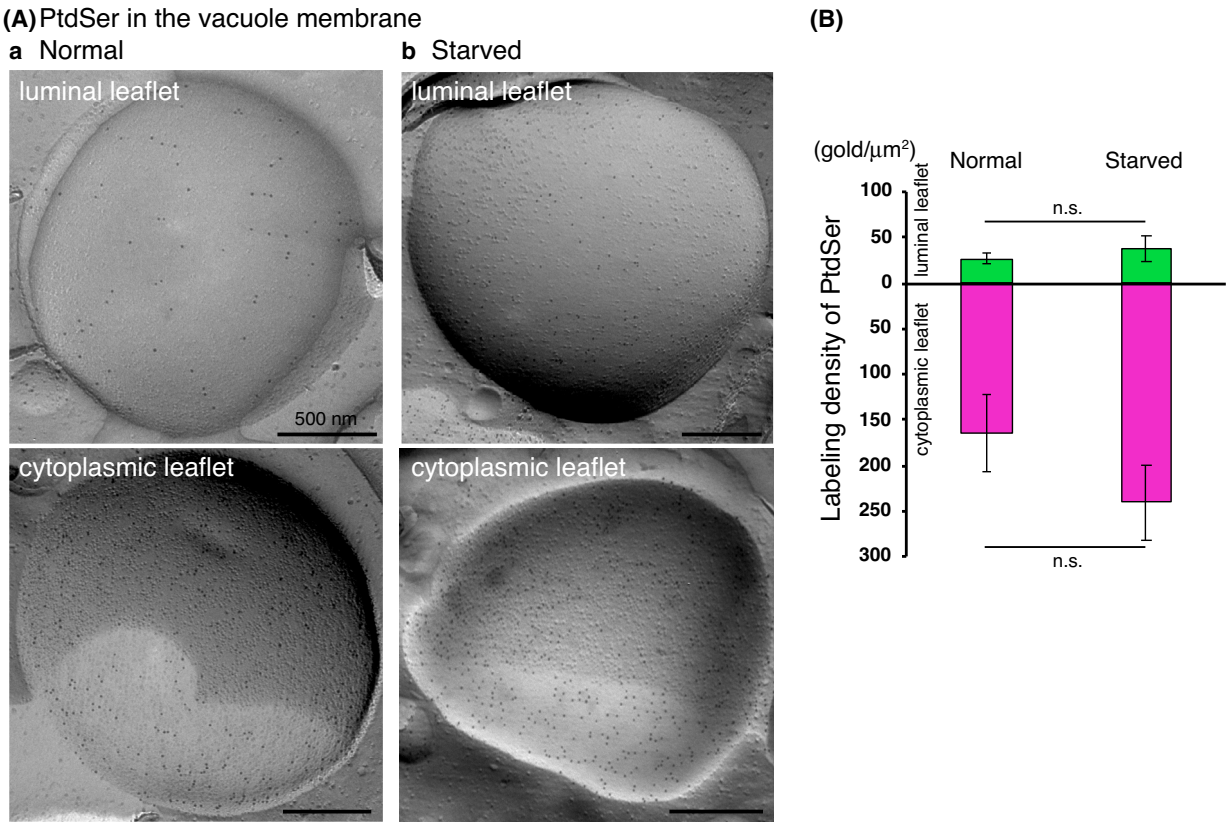


Fig. 4. Labeling of PtdSer in the vacuolar membrane. (A) Microphotographs of the vacuolar membranes in yeast cells in normal growth (a) and starved (b) conditions. The gold labelings of PtdSer were sparse on the EF of the vacuolar membrane in both normal and starved conditions, whereas they were of considerable labelings on the PF in both conditions. (B) Gold labeling densities of PtdSer on the EF (green) and PF (pink) of the vacuolar membrane in the normal (left) and starved (right) conditions. The normal and starved conditions were not significantly different. Data were obtained from three independent experiments.

contrast to PtdIns(4)P and PtdIns(3)P, the labeling of PtdCho (propargylcholine bromide; Fig. 1Ac and Cc) and PtdSer (GST-Evectin-2-PH; Fig. 1Ad and Cd) were detected with similar labeling densities on both EF and PF in the outer and inner autophagosomal membranes. For PtdCho and PtdSer labeling, the results of this study were consistent with those of previous reports [12,13]. Neither autophagosomes nor autophagic bodies were found in autophagy-deficient mutants, deleted with *ATG2*, *ATG3*, *ATG5*, *ATG7*, *ATG8*, *ATG9*, *ATG12*, *ATG16*, *ATG18*, *VPS15*, or *VPS34*, as reported previously (Table S1, data not shown) [7].

Dramatic increment of PtdSer in both EF and PF of the autophagic body membrane in the vacuole

The localization of PtdIns(4)P, PtdIns(3)P, PtdCho, and PtdSer in the autophagic body membrane of the vacuole, which was derived from the inner autophagosome membrane structure, was examined (Fig. 2). As reported previously using the anti-PtdIns(4)P antibody [7], there was mostly no labeling of PtdIns(4)P on both PF and EF of the autophagic body, although few PtdIns(4)P-positive autophagic bodies on the EF were detected (Fig. 2Ab). In contrast, the labeling of PtdIns(3)P (Fig. 2Aa), PtdCho (Fig. 2Ac), and PtdSer (Fig. 2Ad) was constantly observed on both PF and EF of the autophagic bodies in the vacuole. The labeling density of PtdIns(3)P on the PF of the inner autophagosomal membrane was low; therefore, the membrane structures with high labeling density of PtdIns(3)P on the PF were a microlipophagic vesicle (hereafter lipophagic) resulting from microautophagy by the vacuolar membrane, as reported previously (Fig. 2Aa, arrowheads) [14]. In addition, a few membrane structures possess high PtdIns(4)P labeling densities, which are also lipophagic vesicles, as shown previously (Fig. 2Ab, arrowheads; see also Fig. S2) [15].

When the labeling densities of PtdIns(3)P (Fig. 3A), PtdIns(4)P (Fig. 3B), PtdCho (Fig. 3C), and PtdSer

18733468, 2021, 17, Downloaded from https://febs.onlinelibrary.wiley.com/doi/10.1002/1873-3468.14167 by CochraneChina, Wiley Online Library on [02/03/2023]. See the Terms and Conditions (https://onlinelibrary.wiley.com/terms-and-conditions) on Wiley Online Library for rules of use; OA articles are governed by the applicable Creative Commons License

Table 1. Average labeling densities of PtdIns(3)P, PtdIns(4)P, PtdCho, and PtdSer in the autophagosome, autophagic body, and vacuolar membranes. The average gold labeling densities of each lipid on the PF and EF of the autophagosome membrane in the cytosol, autophagic bodies, and lipophagic vesicles in the vacuole and vacuole are shown. n.d., not determined.

Average labeling density (per μm^2) on fracture faces [number of structures]				
Autophagosome	Inner membrane P-face	E-face	Outer membrane P-face	E-face
PtdIns(3)P	54.27 ± 19.75 [14]	386.48 ± 158.75 [3]	25.15 ± 14.68 [4]	370.29 ± 67.54 [13]
PtdIns(4)P	53.87 ± 15.18 [48]	150.96 ± 28.20 [17]	48.09 ± 25.56 [16]	170.82 ± 15.43 [56]
PtdCho	123.49 ± 22.84 [12]	72.16 ± 26.68 [4]	133.39 ± 48.48 [4]	128.57 ± 19.54 [11]
PtdSer	212.82 ± 50.79 [15]	256.02 ± 58.25 [9]	212.14 ± 76.20 [6]	164.17 ± 25.96 [14]

Autophagic body	Wild type P-face	E-face	*atg15*Δ strain P-face	E-face	*pep4*Δ strain P-face	E-face
PtdIns(3)P	32.90 ± 6.04 [35]	356.23 ± 33.40 [42]	n.d.	n.d.	n.d.	n.d.
PtdIns(4)P	9.54 ± 1.99 [120]	21.59 ± 3.60 [101]	n.d.	n.d.	n.d.	n.d.
PtdCho	87.26 ± 13.77 [23]	100.46 ± 22.03 [14]	n.d.	n.d.	n.d.	n.d.
PtdSer	399.84 ± 20.48 [104]	623.83 ± 26.24 [141]	500.18 ± 16.17 [48]	620.23 ± 18.68 [50]	513.32 ± 24.67 [21]	679.84 ± 34.0 [18]

Lipophagic vesicle	P-face	E-face
PtdIns(3)P	211.91 ± 45.02 [17]	61.43 ± 11.24 [16]
PtdIns(4)P	294.37 ± 33.13 [25]	2.14 ± 1.45 [32]

Vacuole	Normal P-face	E-face	Autophagy (5 hr) P-face	E-face
PtdSer	165.61 ± 42.10 [12]	26.03 ± 5.89 [5]	240.34 ± 41.23 [9]	37.29 ± 14.18 [11]

(Fig. 3D) were compared between the autophagosome and the autophagic body, those of PtdIns(4)P (Fig. 3B) and PtdSer (Fig. 3D) dramatically decreased and increased, respectively, in the autophagic body membrane. In contrast to the autophagic body, the labeling densities of PtdSer in the EF of the vacuolar membrane were low in both normal and starved conditions, whereas they were considered high in the PF of the vacuolar membrane under both conditions (Fig. 4; Table 1).

The outer membrane of autophagosomes fuses with the vacuolar membrane in yeast cells, and then, the inner membrane-layered vesicles are concomitantly released into the vacuolar lumen as autophagic bodies. Enzymes in the vacuole selectively degrade the autophagic body membrane derived from the inner membrane of the autophagosome [16,17]. The lipid composition in the autophagic body membrane has not been investigated in detail, despite intense attention to the selective degradation of the autophagic body membrane in the vacuole. For the first time, in this study, we found that PtdSer selectively increased in the autophagic body membrane using the freeze-fracture electron microscopy (EM) method. Atg15/Aut5/Cvt17, the only putative lipase among ATG-related genes, may be involved in the intravacuolar degradation of autophagic bodies [18]. In addition, Atg15/Aut5/Cvt17 has a relatively higher activity in hydrolyzing PtdSer than other phospholipids [19]. In this study, we used phenylmethylsulfonyl fluoride (PMSF) as a proteinase inhibitor, while autophagy was induced in yeast cells. PMSF is a well-known proteinase inhibitor, but it has also been reported to inhibit lipase activity [20]. We labeled PtdSer in the deletion mutant *atg15*Δ yeast strain. Many accumulated autophagic bodies in almost all vacuoles of this deletion mutant were observed, as previously reported [18]. It was found that the labeling level of PtdSer was also high in the membrane of the accumulated autophagic body in the *atg15*Δ yeast, even when autophagy was induced in the absence of PMSF in the S(-NC) (Fig. 5A,C, Table 1). These results suggest that the amount of PtdSer concomitantly increased in the autophagic body membrane when the inner membrane-layered vesicles of the autophagosome turned to the autophagic body in the vacuole. We also examined the labeling of PtdSer in the autophagic body membrane of the deletion mutant *pep4*Δ yeast strain (Fig. 5B and C). It is well known that Pep4p is proteinase A [21,22], which can break down the autophagic body in the vacuole for the reason that many accumulated autophagic bodies are detected in the vacuole of the deletion mutant *pep4*Δ strain [18]. Unexpectedly, the labeling of PtdSer on the EF and PF of

18733468, 2021, 17, Downloaded from https://febs.onlinelibrary.wiley.com/doi/10.1002/1873-3468.14167 by CochraneChina, Wiley Online Library on [02/03/2023]. See the Terms and Conditions (https://onlinelibrary.wiley.com/terms-and-conditions) on Wiley Online Library for rules of use; OA articles are governed by the applicable Creative Commons License

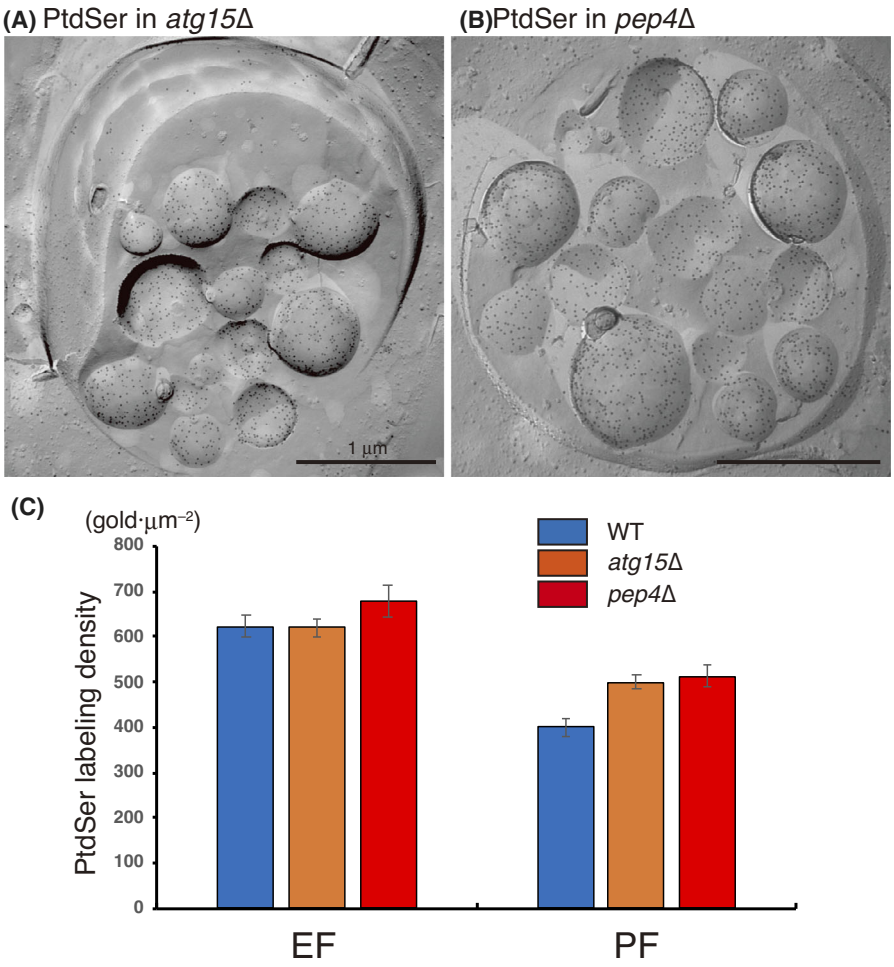


Fig. 5. PtdSer in the membrane of autophagic body in *atg15*Δ and *pep4*Δ strains. Microphotographs of the autophagic body membranes in *atg15*Δ (A) and *pep4*Δ (B) strains are shown. To induce autophagy, *atg15*Δ (A) and *pep4*Δ (B) strain yeasts were cultured in S(-NC) in the absence of PMSF for 5 h. The labeling of PtdSer on the EF and PF of the autophagic bodies in *atg15*Δ and *pep4*Δ strains was comparable to that in the wild-type (WT) yeast. (C) The labeling densities of PtdSer on EF and PF of the autophagic bodies in WT, *atg15*Δ, and *pep4*Δ strains are shown.

the autophagic body membrane in the *pep4*Δ strain was also high, similar to the *atg15*Δ strain, even in the absence of PMSF during autophagy (Fig. 5B,C, Table 1). These results suggest that Atg15p can, in association with Pep4p, degrade autophagic bodies in the vacuole. It is speculated that Atg15p can access PtdSer in the autophagic body membrane to hydrolyze it only after degrading proteins on the surface of the autophagic body by Pep4p because of the steric hindrance by large amounts of proteins.

There is a narrow space between the inner and outer membranes after the autophagosome has been completely formed. PtdSer is thought to be produced in the cytoplasmic leaflet of the outer and inner autophagosomal membrane, and PtdSer is transported to the inner membrane from the outer membrane of the autophagosome or is moved from the cytoplasmic leaflet to the luminal leaflet of the inner autophagosome membrane by transbilayer redistribution. In contrast to PtdSer, PtdIns(4)P dramatically decreased the EF of the autophagic body membrane. Some phosphoinositides, such as PtdIns(4)P, can play roles in transferring lipids through lipid transfer proteins (LTPs) between the membranes of different intracellular organelles; therefore, LTPs have specific links with phosphoinositide metabolism [23]. The PtdSer transporter OSBP homolog 6 (Osh6p) exchanges PtdSer for PtdIns (4)P between the two membranes [24]. However, autophagic bodies in the vacuole were similarly observed in the *osh6*Δ strain (Fig. S3), and the PtdSer labeling on the EF and PF of the autophagic body membranes in the *osh6*Δ mutant yeast were

18733468, 2021, 17, Downloaded from https://febs.onlinelibrary.wiley.com/doi/10.1002/1873-3468.14167 by CochraneChina, Wiley Online Library on [02/03/2023]. See the Terms and Conditions (https://onlinelibrary.wiley.com/terms-and-conditions) on Wiley Online Library for rules of use; OA articles are governed by the applicable Creative Commons License

comparable to those of the wild-type yeast (Fig. S3). With these results, we suggest that PtdSer is transported from the outer membrane to the inner membrane of the autophagosome by mechanisms other than Osh6p. However, we believe that maintaining a PtdIns(4)P gradient at the inner/outer membrane interface could be an important factor for the selective increment of PtdSer in the EF and PF of the autophagic body membrane, which is derived from the inner membrane of the autophagosome. Further studies are needed to understand the mechanisms underlying the increase in PtdSer level in the autophagic body membrane. QF-FRL might be a useful method to investigate them.

Acknowledgments

This work was supported by JSPS KAKENHI Grant Nos JP20H03154, JP17H03935, and JP16K15056 and research grants from the Nakatani Foundation for Advancement of Measuring Technologies in Biomedical Engineering, Takeda Science Foundation, The Naito Foundation, ONO Medical Research Foundation, The NOVARTIS Foundation (Japan) for the Promotion of Science, and The Uehara Memorial Foundation (to AF).

Data accessibility

The data that support the findings of this study are available from the corresponding authors upon reasonable request.

Author contributions

AF conceived the idea. AF supervised the study and designed the experiments. YY, AF, RK, YK, TM, and KF performed the experiments. YY, AF, RK, KF, and YK analyzed the data. AF drafted the manuscript. YK and TM revised the manuscript.

References

1 Mizushima N and Komatsu M (2011) Autophagy: renovation of cells and tissues. *Cell* **147**, 728–741.
2 Matsuda N (2010) PINK1 stabilized by mitochondrial depolarization recruits Parkin to damaged mitochondria and activates latent Parkin for mitophagy. *J Cell Biol* **189**, 211–221.
3 Narendra DP, Jin SM, Tanaka A, Suen DF, Gautier CA, Shen J, Cookson MR and Youle RJ (2010) PINK1 is selectively stabilized on impaired mitochondria to activate Parkin. *PLoS Biol* **8**, e1000298.
4 Narendra D, Tanaka A, Suen DF and Youle RJ (2008) Parkin is recruited selectively to impaired mitochondria and promotes their autophagy. *J Cell Biol* **183**, 795–803.
5 Vives-Bauza C, Zhou C, Huang Y, Cui M, de Vries RIA, Kim J, May J, Tocilescu MA, Liu W *et al.* (2010) PINK1-dependent recruitment of Parkin to mitochondria in mitophagy. *Proc Natl Acad Sci USA* **107**, 378–383.
6 Saitoh T, Fujita N, Ho Jang M, Uematsu S, Yang B-G, Satoh T, Omori H, Noda T, Yamamoto N and Komatsu M (2008) Loss of the autophagy protein Atg16L1 enhances endotoxin-induced IL-1beta production. *Nature* **456**, 264–268.
7 Kurokawa Y, Konishi R, Yoshida A, Tomioku K, Futagami T, Tamaki H, Tanabe K and Fujita A. (2019) Essential and distinct roles of phosphatidylinositol 4-kinases, Pik1p and Stt4p, in yeast autophagy. *Biochimica et Biophysica Acta (BBA)* **1864**, 1214–1225.
8 Fujita A, Cheng J, Tauchi-Sato K, Takenawa T and Fujimoto T (2009) A distinct pool of phosphatidylinositol 4,5-bisphosphate in caveolae revealed by a nanoscale labeling technique. *Proc Natl Acad Sci USA* **106**, 9256–9261.
9 Cheng J, Fujita A, Yamamoto H, Tatematsu T, Kakuta S, Obara K, Ohsumi Y and Fujimoto T (2014) Yeast and mammalian autophagosomes exhibit distinct phosphatidylinositol 3-phosphate asymmetries. *Nat Commun* **5**, 3207.
10 Iyoshi S, Cheng J, Tatematsu T, Takatori S, Taki M, Yamamoto Y, Salic A and Fujimoto T (2014) Asymmetrical distribution of choline phospholipids revealed by click chemistry and freeze-fracture electron microscopy. *ACS Chem Biol* **9**, 2217–2222.
11 Tsuji T, Cheng J, Tatematsu T, Ebata A, Kamikawa H, Fujita A, Gyobu S, Segawa K, Arai H, Taguchi T *et al.* (2019) Predominant localization of phosphatidylserine at the cytoplasmic leaflet of the ER, and its TMEM16K-dependent redistribution. *Proc Natl Acad Sci USA* **116**, 13368–13373
12 Ogasawara Y, Cheng J, Tatematsu T, Uchida M, Murase O, Yoshikawa S, Ohsaki Y and Fujimoto T (2020) Long-term autophagy is sustained by activation of CCTbeta3 on lipid droplets. *Nat Commun* **11**, 4480.
13 Orii M, Tsuji T, Ogasawara Y and Fujimoto T (2021) Transmembrane phospholipid translocation mediated by Atg9 is involved in autophagosome formation. *J Cell Biol* **2**, 20.
14 Tsuji T, Fujimoto M, Tatematsu T, Cheng J, Orii M, Takatori S and Fujimoto T (2017) Niemann-Pick type C proteins promote microautophagy by expanding raft-like membrane domains in the yeast vacuole. *Elife* **6**, 259.
15 Kurokawa Y, Konishi R, Yoshida A, Tomioku K, Tanabe K and Fujita A (2020) Microautophagy in the yeast vacuole depends on the activities of phosphatidylinositol 4-kinases, Stt4p and Pik1p. *Biochim Biophys Acta Biomembr* **1862**, 183416.

18733468, 2021, 17, Downloaded from https://febs.onlinelibrary.wiley.com/doi/10.1002/1873-3468.14167 by CochraneChina, Wiley Online Library on [02/03/2023]. See the Terms and Conditions (https://onlinelibrary.wiley.com/terms-and-conditions) on Wiley Online Library for rules of use; OA articles are governed by the applicable Creative Commons License

16 Baba M, Takeshige K, Baba N and Ohsumi Y (1994) Ultrastructural analysis of the autophagic process in yeast: detection of autophagosomes and their characterization. *J Cell Biol* **124**, 903–913.
17 Takeshige K, Baba M, Tsuboi S, Noda T and Ohsumi Y (1992) Autophagy in yeast demonstrated with proteinase-deficient mutants and conditions for its induction. *J Cell Biol* **119**, 301–311.
18 Epple UD, Suriapranata I, Eskelinen EL and Thumm M (2001) Aut5/Cvt17p, a putative lipase essential for disintegration of autophagic bodies inside the vacuole. *J Bacteriol* **183**, 5942–5955.
19 Ramya V and Rajasekharan R (2016) ATG15 encodes a phospholipase and is transcriptionally regulated by YAP1 in Saccharomyces cerevisiae. *FEBS Lett* **590**, 3155–3167.
20 Kanwar SS, Kaushal RK, Jawed A, Gupta R and Chimni SS (2005) Methods for inhibition of residual lipase activity in colorimetric assay: a comparative study. *Indian J Biochem Biophys* **42**, 233–237.
21 Teichert U, Mechler B, Muller H and Wolf DH (1989) Lysosomal (vacuolar) proteinases of yeast are essential catalysts for protein degradation, differentiation, and cell survival. *J Biol Chem* **264**, 16037–16045.
22 Van Den Hazel H, Wolff AM, Kielland-Brandt MC and Winther JR (1997) Mechanism and ion-dependence of in vitro autoactivation of yeast proteinase A: possible implications for compartmentalized activation in vivo. *Biochem J* **326**, 339–344.
23 Lipp NF, Ikhlef S, Milanini J and Drin G (2020) Lipid Exchangers: Cellular Functions and Mechanistic Links With Phosphoinositide Metabolism. *Front Cell Dev Biol* **8**, 663.
24 Moser von Filseck J, Copic A, Delfosse V, Vanni S, Jackson CL, Bourguet W and Drin G (2015) INTRACELLULAR TRANSPORT. Phosphatidylserine transport by ORP/Osh proteins is driven by phosphatidylinositol 4-phosphate. *Science* **349**, 432–436.
25 Yoshida A, Shigekuni M, Tanabe K and Fujita A (2016) Nanoscale analysis reveals agonist-sensitive and heterogeneous pools of phosphatidylinositol 4-phosphate in the plasma membrane. *Biochim Biophys Acta* **1858**, 1298–1305.
26 Guldener U, Heck S, Fielder T, Beinhauer J and Hegemann JH (1996) A new efficient gene disruption cassette for repeated use in budding yeast. *Nucleic Acids Res* **24**, 2519–2524.
27 Fujimoto T and Fujimoto K (1997) Metal sandwich method to quick-freeze monolayer cultured cells for freeze-fracture. *J Histochem Cytochem* **45**, 595–598.
28 Fujita A, Cheng J and Fujimoto T (2010) Quantitative electron microscopy for the nanoscale analysis of membrane lipid distribution. *Nat Protoc* **5**, 661–669.

Supporting information

Additional supporting information may be found online in the Supporting Information section at the end of the article.
Fig. S1. PtdIns(4)P labeling using GST-OSBP-PH.
Fig. S2. Localization of PtdIns(3)P in the autophagic body membrane and lipophagic vesicle in the vacuole.
Fig. S3. The PtdSer labeling on the PF and EF of the autophagic body membrane in osh6Δ strain.
Table S1. Yeast strains used in this study.

18733468, 2021, 17, Downloaded from https://febs.onlinelibrary.wiley.com/doi/10.1002/1873-3468.14167 by CochraneChina, Wiley Online Library on [02/03/2023]. See the Terms and Conditions (https://onlinelibrary.wiley.com/terms-and-conditions) on Wiley Online Library for rules of use; OA articles are governed by the applicable Creative Commons License